EUSO duty cycle : moon and sun light effects

F. Montanet

LSPC-04-12

EUSO Duty Cycle: Moon and Sun Light Effects

Prepared by: F. Montanet

Approved by: G. D'Ali

Reference: EUSO-SIM-REP-009-1.2

Issue: 1

Revision: 2

Date: April, 2004

EUSO duty cycle: moon and sun light effects

F. Montanet

Abstract:

The major limitation on the EUSO duty cycle comes from the fraction of the time the field of view will be exposed to the sun light or to the moon light. A further limitation could come from the fact that the telescope shutter might have to be closed also when the ISS itself is exposed to either light source. We compute the year averaged duty cycle due to the light-shadow effect under different conditions, taking into account the exact position of the ISS, the sun and the moon minute per minute. This fine time step prediction allows also computing the distribution of the shutter opening times which can be as small as 1 minute.

Note on version 1.2: There is one major correction and one major improvement with respect to the first version of this note which was issued in March 2003:

1. *First of all, there was a very severe mistake in the code used to simulate the phase of the moon. The phase angle was calculated with the wrong sign! Hence, the correlation between the moon phase and the zenith position of both the moon and the sun was wrong. Obviously, when the moon is full, the sun and the moon zenith are anti-correlated, meaning that one of the other is shinning bright up in the sky. During new moon, moonlight is not a problem but the zenith of the moon and the sun are correlated and one does not gain anything by accepting moonlight background. The only gain comes from the moon close to the horizon during the half moon periods. The conclusion of the first version was in contradiction with this naïve reasoning.*
2. *The model of the atmosphere used in the first version was over simplistic. It was assumed to act as a thin layer lambertian diffuser (uniform radiance or constant albedo with respect to the moon zenith angle). It was realised that this is probably not realistic. Again, naively, the clear atmosphere is a thin layer with a characteristic scattering length which is big compared to the vertical depth. On the other hand, the ground albedo is small compared that of the atmosphere. A more realistic representation of the atmosphere + ground is something in between the quasi-lambertian model first used and a thin milky layer on top of a black surface. The consequence of this is that at big zenith angles (low elevation), the moonlight will travel longer path in the atmosphere and will have more chance to scatter. It is expected that the albedo and the radiance actually increase with the zenith angle, reaching a maximum and then dropping because of the attenuation of the incoming flux. This is confirmed by using the COART model (LOWTRAN + a sea surface model as an additional layer – see: http://snowdog.larc.nasa.gov/jin/rtset.html), obtaining the full BDRF of the atmosphere plus the oceanic surface and integrating it on the EUSO solid angle. In this version we incorporate this new moon zenith angle dependence of the moonlight background flux. The COART model does not account for "twilight" effect. This was added by hand as an exponential dependence according to Tyson and Gal (Astrom J 105 (3) '93).*

Introduction:

Very roughly half of the time, EUSO will be overlooking night and during about half of that time, will the moon be above the horizon. Averaging on the sun and the moon positions, neglecting moon phases, this gives a crude 25% upper limit for the detector duty cycle. Obviously, at new moon, the background light might be sustainable up to a certain level and the moon phases have to be taken into account in some way.

On the other hand, it is unclear whether the telescope will be able to operate when exposed to direct light from either the sun or the moon, even if the field of view is well in the dark. As a matter of fact, because of the ISS high altitude (~ 400 km), it enters or exit the umbra cone when the sun or the moon are still 19.8° below the horizon at sea level.

Estimating the background light level in these conditions is difficult, because it depends both on the possible stray light from parasitic reflections on the telescope baffle, as well as on large angle scattering on the rarefied gas surrounding and below the ISS. The results presented in this note will therefore make the hypothesis that the ISS should be **out of direct sunlight**. This naively reduces the duty cycle to $\left[(180° - 2\times 19.8°)/360°\right] = 39\%$, for the sun only instead of 50%. This also accounts for the "twilight" period during which the atmosphere above the field of view (FOV) is still too luminous.

In fact, it is important to realize that even this naive calculation is wrong. It is based on an idealized situation, neglecting the variation of the orbit inclination with respect to the ecliptic plane, as well as its orientation with respect to the sun illumination. As we will see, a detailed calculation shows that there are periods of time during a sideral year when the ISS is constantly in the sunlight. The year averaged duty cycle due to sunlight is found to be **34.25%** instead of 39%.

As far as the moon is concerned, we have chosen two different hypotheses:

1. A strict cut as for the sun for which observation time is restricted to the moon being below the ISS horizon, namely with a zenith angle bigger than 90°+19.8° = 109.18°, whatever the moon phase is.
2. A less stringent cut assuming that a fraction of the time when the moon is above the horizon, say at new moon for example, the background will be low enough to be acceptable. The background is evaluated using a rough estimate of the flux of background light backscattered by the ground and the atmosphere, depending upon the moon zenith angle and phase angle. We have recently refined this estimate by using a complete atmosphere simulation using the COART model (see below).

For the purpose of this calculation, we have chosen to compute for each time step, the relative positions of the ISS, the sun and the moon, minute per minute for a year long period. From these positions, one can obtain the actual crossing time of the earth umbra cone with a 1 minute precision as well as the moon phases.

Ephemerides

We have used the SLALIB positional astronomy library [1] to compute the pointing vectors to the sun and to the moon centre. SLALIB is a very accurate and complete set of routines to compute positions of solar system or stellar objects, convert between coordinate systems or calendars etc. It provides much more functionalities and accuracy than really needed here but it is simple enough to use and shortcuts a lot of complex coding (and mistakes that usually follow).[1]

[1] Unfortunately, FORTRAN coding had to be used, because although it is possible to interface SLALIB to C, the publicly available version of the library has not yet been ported to C or C++.

We first define the time and date in the Modified Julian (MJ 2000) calendar and compute the moon and the sun position in the fixed equatorial coordinate system (i.e. right ascension α, declination δ). Using the time and the observatory position (the ISS longitude, latitude and height, see bellow), the equatorial coordinates are then transformed to local (geodetic) horizon coordinates, namely azimuth Az and elevation El or zenith angle θ_Z .

The sun and the moon eclipse times are then defined using a simple cut on the zenith angle:

- ISS in the umbra $\theta_Z > \pi - \arcsin(R/(R+H)) = 109.18°$
- ISS in the light $\theta_Z < \pi - \arcsin(R/(R+H))$

where *R* is the earth radius and *H* the ISS height above ground level.

Computing the ISS position

The a first approximation, the trajectory of the ISS is a geosynchronous orbit, obviously a keplerian ellipse, inclined 51° with respect to the equatorial plane. This ellipse is rotating around the pole axis in the solar inertial frame with a precession period of roughly 72 days.

In real life, things are considerably more complicated. On top of the main central forces, many additional perturbations have to be taken into account if one wants to be able to accurately predict the position of the satellite. These additional forces will act to change our satellite's orbital path from that of a true ellipse. First of all, the earth is not a point mass because of its oblateness and because of its non uniform density. Furthermore, one cannot, ignore the gravitational effects of the sun and the moon. There are non-gravitational forces to consider as well. The primary one is due to the rather low-earth orbit of the ISS and because of its large span which cause the atmospheric drag to act as a non-negligible dissipative force.

Ignoring these perturbations for a low-earth orbit will result in significant errors. One of the main effects is that the ISS is “falling” gradually down, at a rate of roughly 11 km in 100 days.

A large literature exists on the theory of the motion of artificial earth satellite and numerous models have been worked out that aim at predicting satellites positions mostly using unfolding of perturbations effect, like the one we used: the NORAD SGP model. During the 1970s, NORAD (the North American Aerospace Defence Command) developed a fully-analytical orbital model. With this model, known as SGP (for Simplified General Perturbation), a user can calculate a satellite's position and velocity at a particular time directly, without the need for numerical integration. The result is a considerable reduction in computational burden to support tracking the growing population of earth-orbiting satellites.

NORAD maintains general perturbation element sets on all resident space objects. These element sets are periodically refined so as to maintain a reasonable prediction capability on all space objects[2]. In turn, these element sets are provided to users (historically in a compact 2 line format sets called Two Line Elements or TLE). In a publicly available report [2], NORAD summarises the method of propagating these element sets in time to obtain a position and velocity of the space object and even provides the FORTRAN code to do so. We have used the code listed in this report as templates and have re-written a set of routines in FORTRAN as well as in C++ to compute the ISS position for any MJ date, starting from the ISS Two Line Elements. TLE sets can be fetched from different ftp or web sites and are updated daily.

This piece of code has been tested in different ways, but one of the most stringent tests was to calculate in real time the current position of the ISS and to compare the longitude and latitude obtained to those provided by one of the many real time software’s available on the internet.

[2] Note that in the case of the ISS, it is of vital importance to use updated TLE’s due to the fact that the station has to be pushed up regularly by the shuttle to compensate for the decay of its orbit!

For example, the agreement with the well spread and GNU licensed "Predict"[3] software was found to be within a fraction of a degree.

Moon phases and background

Moon magnitude phase curves:
The moon does not act as a simple lambertian spherical reflector and taking it as such would lead to large errors. Among other things, it has much stronger phase dependence, shows almost no limb darkening and presents a strong opposition effect. It is therefore unavoidable to use an empirical model fitted to real photometric data.
Many models of the moon brightness have been proposed, mostly in the seventies, when both precise photometric data and surface samples became available. Complex bi-directional reflectance functions have been fitted to the data and analysed to extract information on the nature of the moon powder like soil. The same kind of analysis is still being actively pursued to study the nature of other solar system asteroids and satellites.
Many measurements and parameterisation of the relative brightness of the moon as a function of the phase angle are available. The basic phase curve is rather simple but deviates quite significantly from that of a straightforward lambertian sphere. The magnitude ($\log_{10}(2.5\times \mathrm{Ir})$) is quasi linear with the phase angle α for angles between 7° and 30°. For larger angles the phase curve is best fitted with a biquadratic form of the type:

$$\mathrm{mag} = \mathrm{mag}_0 + a_1|\alpha| + a_4\,\alpha^4,$$

where $\mathrm{mag}_0 = -12.73$ is the absolute magnitude of the full moon, $a_1 = 1.5$ and $a_4 = 4.3\times10^{-2}$ if the phase angle α is expressed in radians (-π to π) [3]. The half moon is about 10 times less luminous than the full moon. One should stress that although this model agrees quite well with photometric measurements its accuracy for phase angle close to π (new moon) is probably not very good. There are also three noticeable deviations between the data and this parameterisation, which will all be neglected in the following:

- At small angles (± 7° around the full moon), photometric data show a sharp increase in the moon brightness. The full moon is about 35% brighter than the above model or a simple extrapolation would predict. This is known as the opposition effect and is interpreted as due in part to a shadowing effect (surface roughness casting shadow reducing reflectivity except near zero phase), and to a coherent effect depending upon the size of the dust grains and on wavelength.
- Another deviation is a before-after full moon asymmetry the moon irradiance is slightly less after full moon than before full moon for symmetric phase angles. This is due to a larger proportion of darker "mare" in the western part of the moon face.
- A third effect is known as the *earthshine*. This is the faint light visible on the dark side of the moon when it is a thin crescent. Earthshine depends strongly on the phase of the Earth. When the Earth is full (at new Moon), it casts the greatest amount of light on the Moon, and the earthshine is relatively bright and easily observed by the naked eye. At exact new moon, the earthshine effect is about 1.5×10^{-4} less luminous than the full moon. The above function drops down to 2.7×10^{-4} of the value of the full moon and seems to slightly overestimate the moonlight flux at large phases.

[3] http://www.qsl.net/kd2bd/predict.html

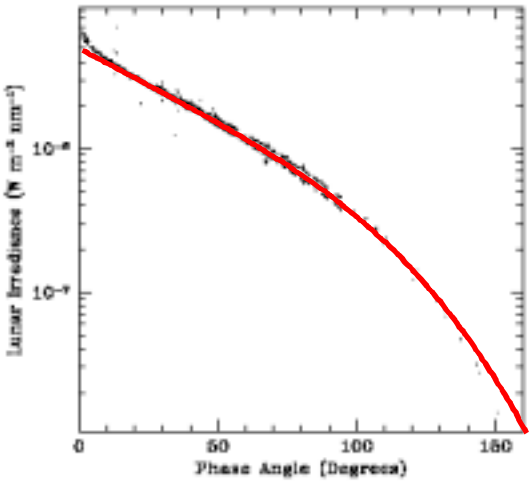

Figure 1: Lunar absolute irradiance at 555 nm as a function of the moon phase from the ROLO photometric measurements [5]. The strong phase dependence, the opposition effect, the east-west asymmetry are clear seen. The simple parametric phase curve from [3] is overlaid in red for comparison.

For our purpose of computing low illumination background what matters mostly is to predict with some accuracy the moonlight at large phase angles (near new moon). Although data at large phase angle are rare, the phase dependence above does a fairly good job down to 120° and the comparison with earthshine data indicates that if anything, it overestimates slightly the large phase irradiation.

Lunar irradiance modelling:

Converting a relative magnitude to a photon flux in a given spectral range requires the knowledge of a precise photometric calibration. The moon has been often used as a calibration source for photometric instruments but absolute calibration data in the 300-400 nm range are scarce. The most relevant radiometric information we could find comes from the ROLO program (a terrestrial robotic lunar observatory) [5]. Observation are routinely made since 1996 over a range 350-950 nm using 23 passband filters, correcting for the atmosphere attenuation and normalising the data to bright stars of known magnitude. The magnitude as function of the phase at 555 nm is shown in Figure 1 and is compared to the parametric function from [3] which compares quite well. The 555 nm phase curve is extrapolated to 0° phase (full moon) neglecting the opposition effect with the aim of setting an absolute irradiance normalisation: The full moon (linear extrapolation neglecting the opposition effect) corresponds to:

$$Ir_{555} \approx 5\times10^{-6}\ W/m^2/nm \ \text{ at } \ 555\ nm$$

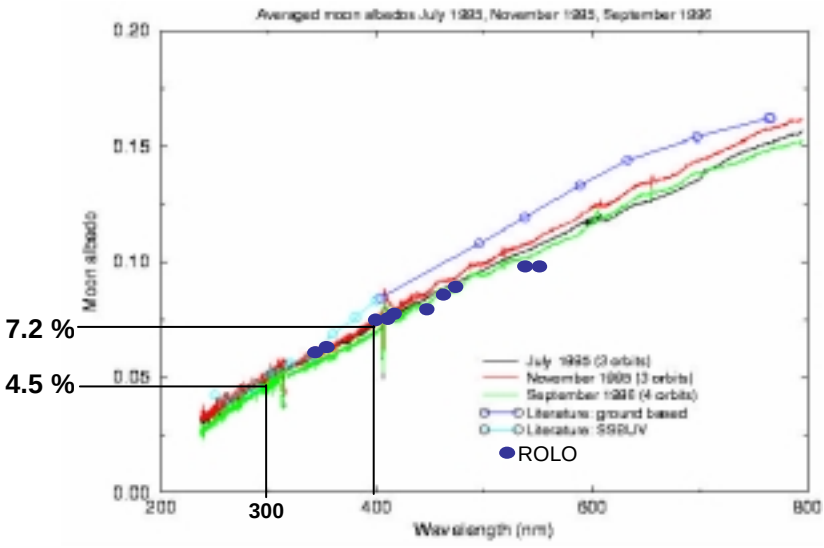

Figure 2 : The spectral variation of the moon albedo from the GOME moon measurements and from the ROLO measurements.

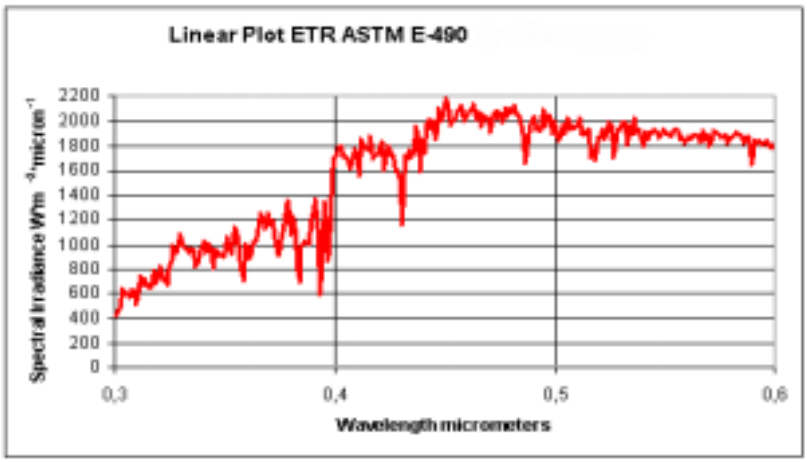

Figure 3 : The top of atmosphere absolute solar irradiance in the 300 to 600 nm

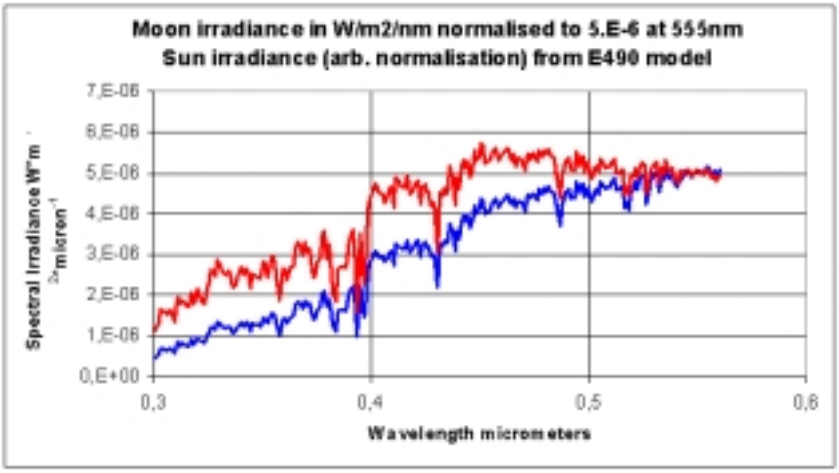

Figure 4 : The absolute moon irradiance as a function of wavelength in blue. It was computed from the solar irradiance normalised to 5×10^{-6} W/m²/nm at 555 nm (in red) times the moon albedo.

Absolute irradiance of the moon at 350 nm was harder to find in the literature. We have therefore estimated the irradiance at 300-400 nm by taking into account the variation from

555 nm to 350 nm of both the solar irradiance and of the moon reflectance. Standard solar spectra show a sharp drop from above to below 400 nm and a rather flat irradiance spectrum between 300 and 400 nm. The ratio of the averaged irradiance between 300 and 400nm is close to on half of its value around 555 nm (Figure 2).

Reference [3] and [4] gives the relative reflectance of the moon for different narrow band filters normalised to 555 nm. The reflectance drops almost linearly from 1 at 555 nm to 0.62 at 350 nm. The irradiance of the moon averaged in the range 300 to 400 nm is thus assumed to be:

$$\mathrm{Ir}_{350} = \mathrm{Ir}_{555} \times \int_{300\,\mathrm{nm}}^{400\,\mathrm{nm}} \frac{A(\lambda)}{A(555\,\mathrm{nm})} \times \frac{\mathrm{Isun}(\lambda)}{\mathrm{Isun}(555\,\mathrm{nm})} d\lambda = 1.33 \times 10^{-7}\ \mathrm{W/m^2}$$

We can than define the photon flux from the full moon at the top of the atmosphere by integrating $\Phi_0(\lambda)$ over the range 300 to 400 nm:

$$\Phi_0 = \mathrm{Ir}_{555} \times \frac{1}{100\mathrm{nm}} \times \int_{300}^{400} \frac{A(\lambda)}{A(555\,\mathrm{nm})} \times \frac{\mathrm{Isun}(\lambda)}{\mathrm{Isun}(555\mathrm{nm})} \times \frac{\lambda}{1240(\mathrm{ev/nm})} \times \frac{10^{-9}(\mathrm{ns/s})}{1.6 \times 10^{-19}}\, d\lambda$$
$$= 2.437 \times 10^5\ \ \gamma_{300-400}/\mathrm{m^2/ns}$$

Hence, the flux dependence as a function moon phase is given by the empirical expression:

$$\Phi(\alpha) = 2.437 \times 10^5 \times 10^{-0.4\left(1.5|\alpha| + 4.3 \times 10^{-2}\alpha^4\right)}\ \ \gamma_{300-400}/\mathrm{m^2/ns}$$

were α is the phase angle in radians.

Moonlight background:

According to simulations [6], the reflection of UV light on the earth is mainly due to the atmosphere. Assuming a clear sky atmosphere with a total transmission of 0.4 and a surface albedo of 0.1, the fraction of an incoming isotropic light flux which is scattered upward by the atmosphere is ~35%, the rest (~65%) is transmitted-scattered downwards. From this ~65%, only 7% is reflected by the ground, and 5% is transmitted to the top of the atmosphere. The total albedo is thus ~40%. In the case of moonlight, the situation is complicated by the fact that the incoming beam is not isotropic but unidirectional.

We first assume that the atmosphere acts as an isotropic diffuser, so that the Bond Albedo A is independent off the incoming light direction and the elementary flow $d\phi_{\mathrm{moon}}$ emitted by an elementary surface dS of atmosphere is given by:

$$\phi_{\mathrm{Moon}} = \iint \frac{\Omega}{2\pi} A \cos\theta\, \Phi(\alpha)\, dS = \frac{A\cos\theta}{2\pi} \Phi(\alpha) \iint \Omega\, dS$$

where $\cos(\theta)$ is the moon zenith angle cosine, and $\iint \Omega\, dS$ is the solid angle of EUSO. Then, the Moon background in $\mathrm{photons/m^2/ns/sr}$ in the 300-400 nm range is:

$$BG_{Moon}(\theta,\alpha) = \frac{A\cos\theta}{2\pi}\Phi(\alpha)$$
$$\approx 1.55 \times 10^4 \times \cos\theta \times 10^{-0.4\left(1.5|\alpha| + 4.3\times10^{-2}\alpha^4\right)}\ \ \gamma_{300-400}/m^2/ns/sr$$

In other words, the full moon at the zenith of EUSO would produce ~15500 photons/m^2/ns/sr. If one consider 2.5 µs time bins (GTU), this corresponds to the following rate in photoelectrons per pixel and per GTU (assuming 5% for the photon conversion efficiency and optics transfer, 5m² for the aperture and $\approx 4.2\times10^{-6}$ sr / pixel):

$$BG_{Moon}(\theta,\alpha) \approx 40\times\cos\theta\times10^{-0.4\left(1.5|\alpha|+4.3\times10^{-2}\alpha^4\right)} \; pe/pixel/2.5\mu s$$
$$\approx 3.6\times\cos(\theta)\; pe/pixel/2.5\mu s \quad \text{at half moon}$$
$$\approx 0.4\times\cos(\theta)\; pe/pixel/2.5\mu s \quad \text{at quarter moon}$$
$$\approx 1\times10^{-4}\cos(\theta)\; pe/pixel/2.5\mu s \quad \text{at new moon}$$

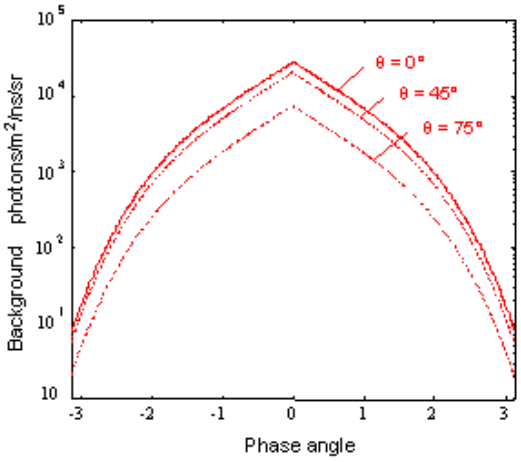

Figure 5: Background photons induced by moon light only, in the EUSO acceptance as a function of the moon phase angle and for different moon zenith angles.

Using a refined atmosphere model

There is no reason that the atmosphere actually acts as a Lambertian diffuser. On the contrary, because of longer path length and because the diffusion length is longer or comparable to the vertical depth, one expect on the up-welling radiance to increase with the moon zenith angle. We have used the "Coupled Ocean and Atmosphere Radiative Transfer" (COART) model to compute top of atmosphere radiances with realistic mean atmospheric conditions above the ocean. COART is a tool available on the web (http://snowdog.larc.nasa.gov/jin/rtset.html) that calculates the radiances and irradiances (flux) at any levels in the atmosphere and ocean [?]. We have obtained top of atmosphere (100 km) upwelling radiances in W/m²/µm/sr integrated in the spectral range 300 – 400 nm spectral. The incoming irradiance was that of the sun at different solar zenith angle. The atmospheric model was a mid-latitude summer model with a boundary layer aerosol model maritime from MODTRAN with no stratospheric layer aerosol and with two different nebulosity situations: clear sky i.e. no cloud and a layer with opacity of 10 and a cloud top at 3 km. The total aerosol loading was confined by aerosol optical depth(500nm) = 0.20. The ocean surface was modeled using the following input parameters : a wind speed of 7 m/s, an ocean depth of 1000 m with a bottom albedo of 0.2, a Chlorine content of 0.2 mg/m^3 and the default ocean particle scattering function (Petzold Average(bb/b=0.0183)). The top of atmosphere upwellig radiances were obtained for 8 equally spaced azimuthal angles and for zenith angles every 5° from 0 to 30°. It was integrated over the EUSO solid angle using linear interpolation between these points. The resulting integrated

radiance was then normalized to the solar incoming irradiance to obtain the partial albedo in the EUSO solid angle, as a function of the solar zenith angle. The resulting albedo variation as a function of the solar (moon) zenith angle is shown in Figure 6. The resulting moonlight flux at the EUSO detector was then obtained using the flux normalization as described above taking into account the albedo zenithal dependence (Figure 7).

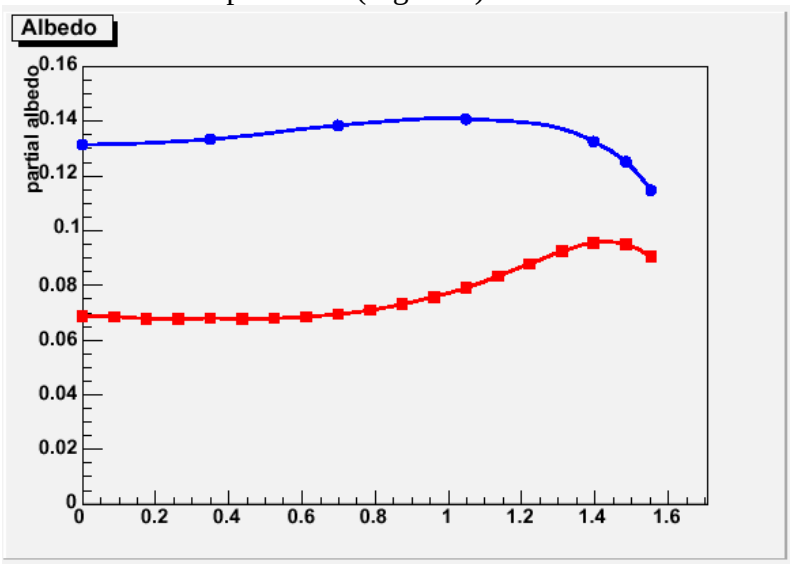

Figure 6 : The partial albedo (in the 0-30° detection cone of EUSO) as a function of the moon zenith angle. The expected increase of the fraction of moonlight scattered at large zenith angle is clearly seen. In red, clear sky (no cloud) ; in blue, uniform cloud layer with opacity of 10 and top at 3km.

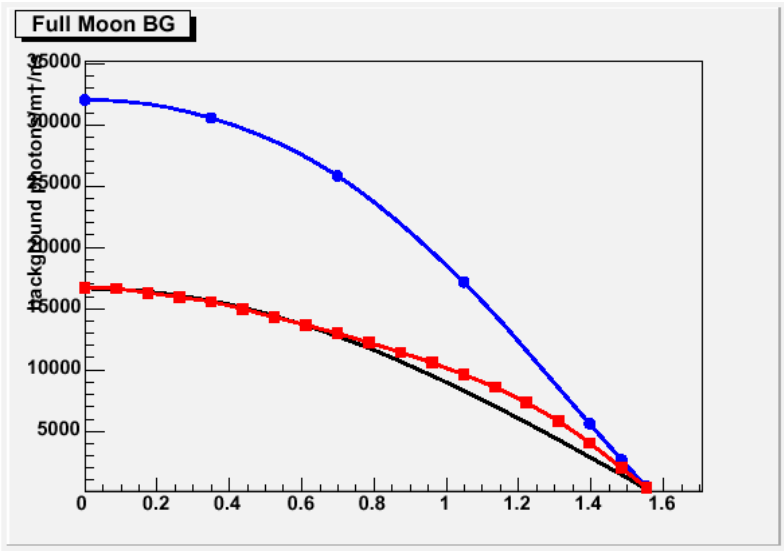

Figure 7 : The full moon induced background flux at the detector as a function of the moon zenith angle using the zenith angle dependence deduced from COART (in red clear sky, in blue with clouds). The black curve is the flux assuming no zenith angle variation of the albedo (only a cosine dep. from the projection angle).

The COART model does not account for doubly scattered light as it would be necessary to reproduce the twilight effect. The radiance is zero if the sun is below the horizon. We have looked for model of the twilight as a function of the time after sun-set or as a function of the zenith angle. This kind of parameterisations is useful to astronomers to define possible extended observation times and night sky background condition for bright object observation. A convenient parameterization is given by Tyson and Gal (Astrom J 105 (3) '93). The twilight sky background variation is rather independent of the observation angle for angles close the

zenith. The background light flux drops exponentially with time after sun-set with a time constant which is latitude and season dependant (time is of course related to the depression angle (zenith angle – 90°) and to the latitude of the observer). On the other hand, the zenith angle dependence is instead quasi independent of the observer latitude and of the season. We found that the parameterization from Tyson and Gal can be conveniently replaced by a simple zenith angle dependence:

$$BG(\theta_{dep}) = BG_{89^\circ} \times 10^{-0.36 \times \theta_{dep}}$$

where BG_{89° is the background at 89°

and θ_{dep} is the depression angle in degree($\theta_{zenith} - 90^\circ$)

Instead of setting the moonlight background to zero for zenith angle below the horizon, we use this sharp roll off (factor 1000 in 8'20" at the equator and at the equinox).

Putting everything together

Using the previously described procedure, we compute for a year long period and minute per minute, the position of the ISS, the zenith angle of the sun and of the moon at this position and time, and the moon phase α. The moon light flux and the moon background are then estimated from the above formulae. The decision is then taken to open or close the shutter depending on the selected criterion: a) moon and sun hidden, or b) sun hidden and moon background below the limit. The length of the exposures is then computed, summed and counted, day by day and year long statistics are produced.

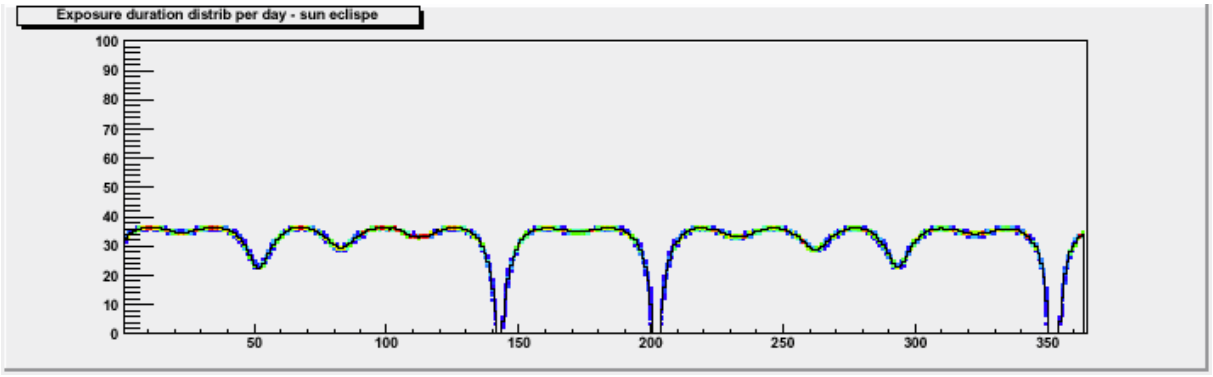

Figure 8 : Distribution of the exposure durations in minutes for each day in one year if the sun only is taken into account. The periods when the exposures are dropping to zero correspond to the days when the orbit axis is almost aligned with the sun direction.

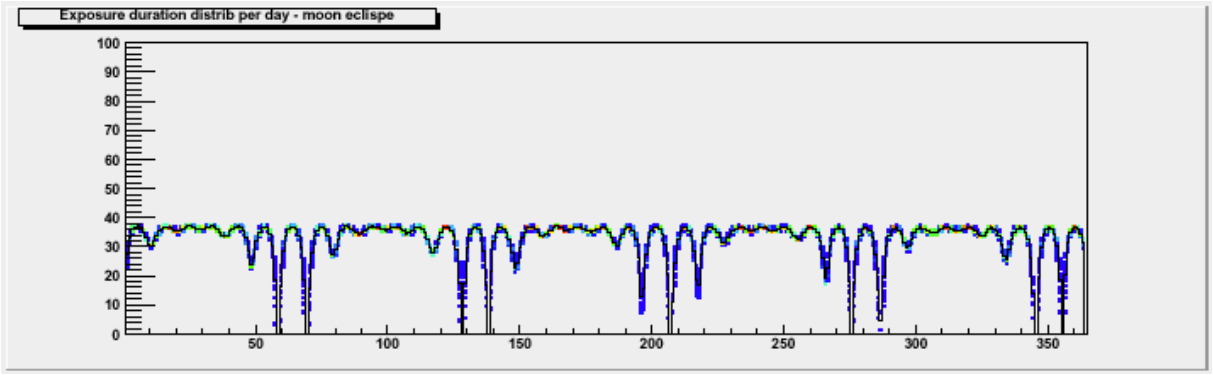

Figure 9: The same distribution but this time taking only the moon into account by requesting it to out of sight. Again, there are periods when the orbit is facing the moon and when data taking will be impossible.

Figure 8 and Figure 9 show the distribution of the exposure period durations for each day for one year. Figure 10 shows the day averaged duty cycle (fraction of active time during one day) for one year if one only takes the sun into account. One realize looking at these curves that because of the precession of the orbit, there are a two to three periods of a few days during in one year when the orbit axis is almost aligned with the sun direction. This means that these periods are completely lost for data taking. This effect reduces the naïve 39% duty cycle due to the sun only to a more realistic 34.6%. The same phenomenon is also true for the moon if it is required to be eclipsed. Note that an analytic description of these fancy curves can be easily produced using a simplified model of the orbit and earth rotation.

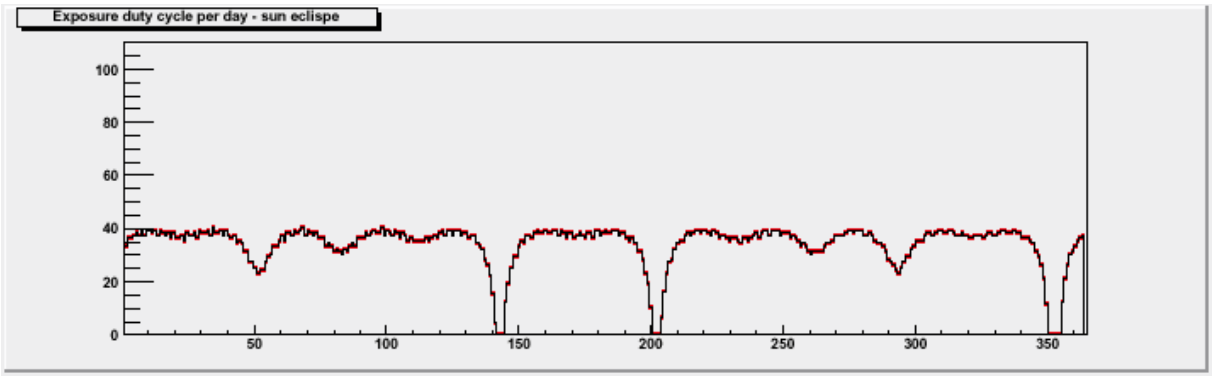

Figure 10 : The day averaged duty cycle in percent (fraction of active time during one day) for one year if one only takes the sun into account.

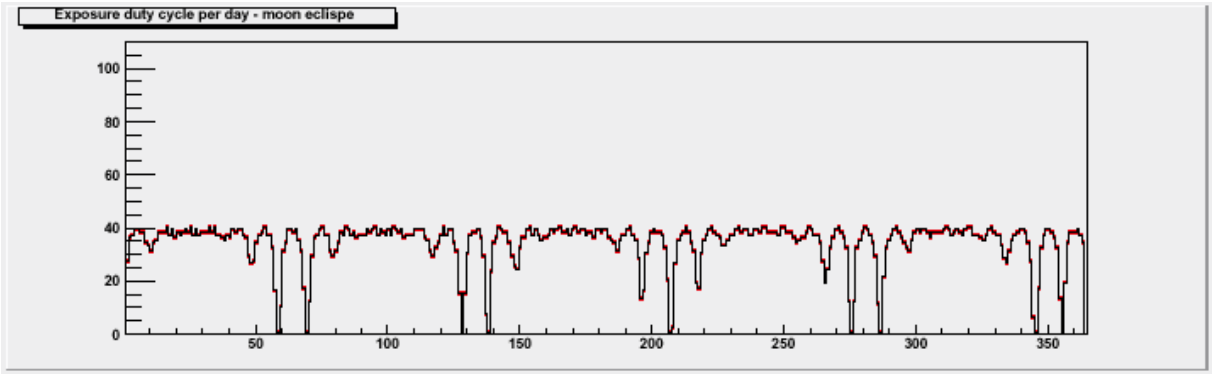

Figure 11: The day averaged duty cycle in percent (fraction of active time during one day) for one year if one only takes the moon into account requiring it to be hidden (θ_{zenith} > 109.18°).

Figure 11 shows the day averaged duty cycle for one year only taking the moon into account and requiring it to be hidden (θ_{zenith} > 109.18°).
The moon background as a function of the day is shown in Figure 12. Only the envelope of the background curve is visible, the actual curve oscillate with a period corresponding to the orbit revolution between zero and the maximum of the curve as seen in the inlet on the same picture. Accepting some additional background light from the moon enables to run longer periods in the valleys of this histogram. Figure 13 shows the same variables than Figure 11 but accepting up to 100 photons/m^2/ns/sr from moonlight.

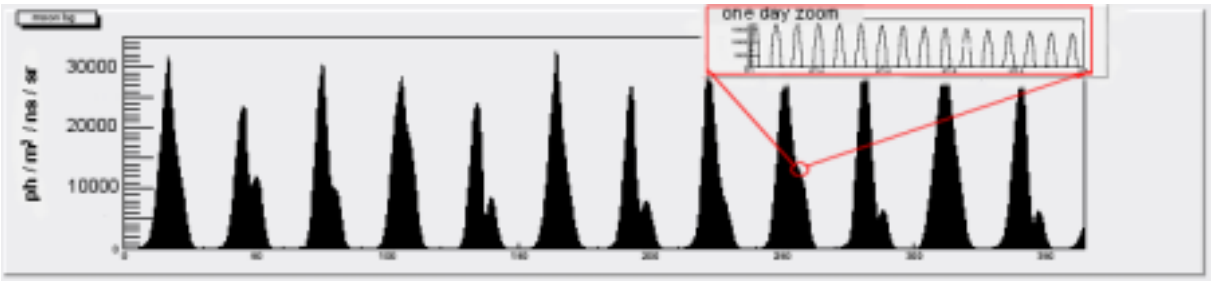

Figure 12: The moonlight induced background in 1 minute bins for one year. The inlet shows a one day zoom where the cos(θ) modulation of the ~15 orbits can be seen.

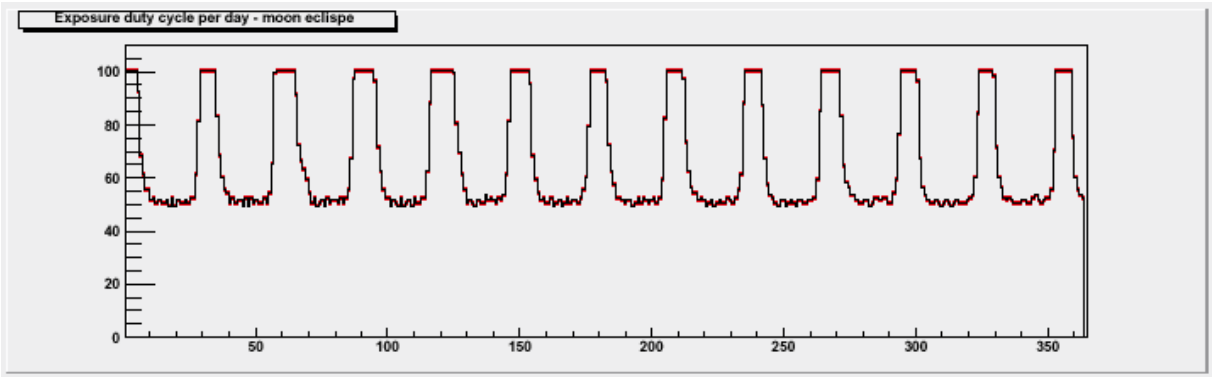

Figure 13 : The day averaged duty cycle in percent (fraction of active time during one day) for one year if one only takes the moon into account asking that the moonlight background is < 100 photons/m^2/ns/sr.

Of course, both conditions on the sun and the moon have to be combined. This is again done on a minute per minute basis. This is necessary because of the strong correlation effects between the moon phase and the zenith angles of the sun and the moon. shows the day averaged duty cycle for one year asking the sun and the moon to be hidden (both $\theta_{zenith} > 109.18°$, in black in), and accepting increasing amount of moonlight induced background (1, 100, 200 and 500 photons/m^2/ns/sr). Basically, except around new moon, when the sun is up the moon is down and vice versa. If one asks both the sun and the moon to be below the horizon, there is a large fraction of the year, **119 full days**, when either one or the other of the two light sources will prohibit running the detector. The year average duty cycle with these strict conditions is only **13%.** This anti-correlation also explains why the duty cycle increases only slowly when accepting more moonlight background.

Note that there is a fraction of that time when the moon is below the horizon but already visible from the ISS ($90° < \theta zenith < 109.18°$). If one assumes that the background induced by the moon light in the atmosphere is negligible for this transition period, one can extend the running time quite a lot and almost for free (from 13% to 17.96%, from black to red in Figure 14).

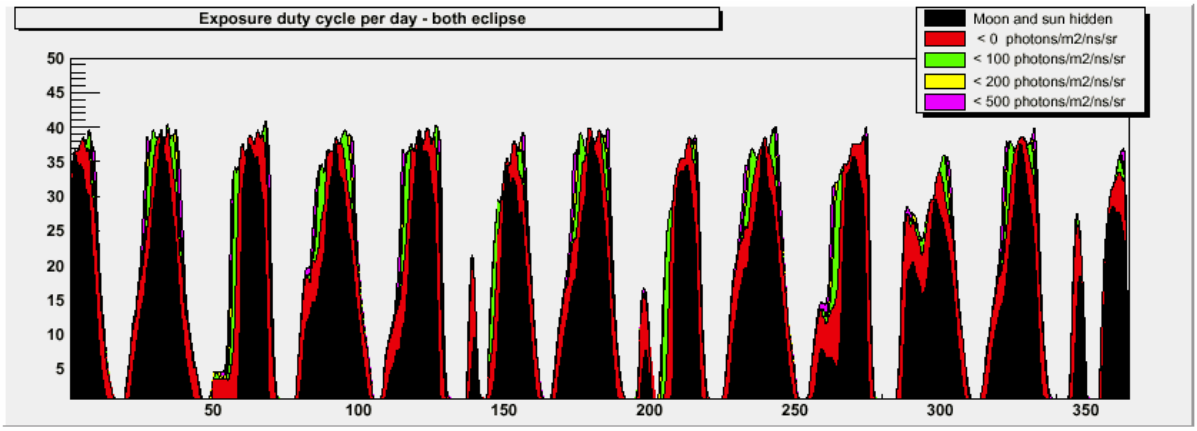

Figure 14: The day averaged duty cycle for one year asking the sun and the moon to be hidden (both θ_{zenith} > 109.18°, in black), and accepting increasing amount of moonlight induced background (0 or quasi-null, 100, 200 and 500 photons/m^2/ns/sr).

Of course, a more refined moonlight "twilight" simulation should be developed. The main other backgrounds are the airglow (~300-600 photons/m2/ns/sr), the Zodiacal Light (~180), diffuse star light and planets (~190). The values for the year average duty cycle with different background conditions are summarized in the

Table 1 and the background limit dependence is shown in Figure 15.

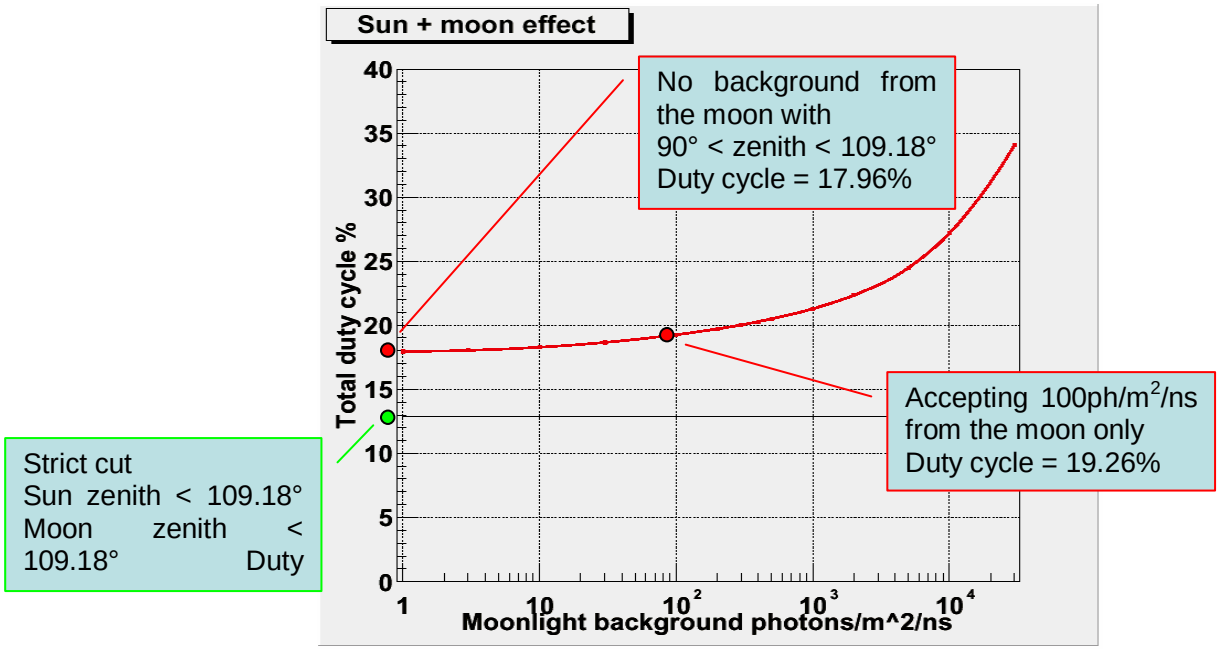

Figure 15: The year average duty cycle as a function of the moonlight induced background limit.

Table 1 : The duty cycle for different background conditions.

Moonlight induced background limit		Sun zenith > 109.18°	Moon effect only	Moon +Sun
photons/m^2/ns	photoelectrons/pixel/µs	%	%	%
Moon zenith > 109.18°		34.25	34.60	13.00
1	7×10^{-4}		51.23	17.96
3	2×10^{-3}		51.21	18.05
10	7×10^{-3}		56.12	18.28
30	0.02		60.96	18.65
100	0.07		66.27	19.26
200	0.15		69.35	19.72
300	0.22		71.10	20.03
400	0.30		72.30	20.28
500	0.37		73.25	20.50
1000	0.75		76.34	21.29
2000	1.5		79.78	22.35
5000	3.7		85.87	24.47
10000	7.5		91.85	27.18
30000	22		99.85	34.10

Opening time distribution:

Another byproduct of this study is the distribution of the opening times (). The shutter protecting telescope will require some time for opening and closing. This implies that short periods of exposure will be problematic or completely lost. One sees from that another drawback of using a stringent cut for the moon is that a large fraction of the active time consists of very short openings (~1/3rd of the openings are shorter than 10 minutes adding up to 8.6 % of active time).

If one accepts 100 photons/m^2/ns/sr, this fraction drops to 5.8 % of the active time and 10 % of the opening. From the figure, one can see that when accepting even a small amount of background, shorter openings are concatenated together and that the peak at 35.80 minutes long openings (the longest time for the ISS to travel through the umbra) has increased quite a lot.

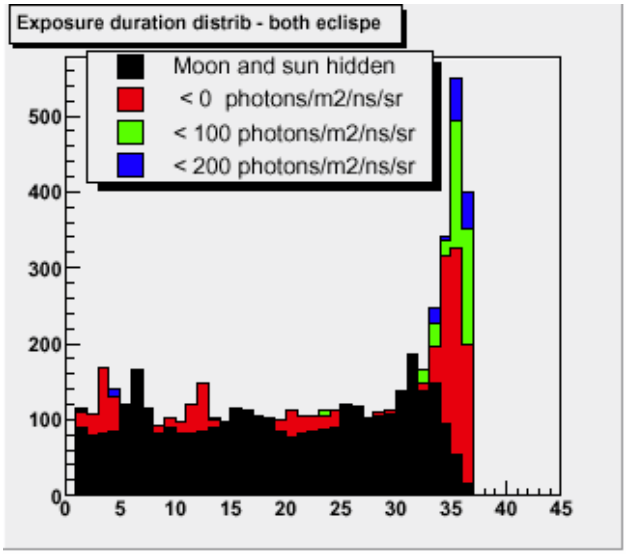

Figure 16: The distribution of the individual exposures durations (or opening times). This shows the number of openings as a function of there duration.

Conclusions

In conclusion, we have shown that the average duty cycle for EUSO due to the sun and moonlight is 12.86% if both the sun and the moon are requested to be safely below the horizon from the ISS. Accounting for the variation of the moonlight flux with the moon phase angle, and computing the moonlight fraction reflected by the earth atmosphere, one can estimate the additional background induced by moonlight. Accepting even a quasi negligible additional background allows to improve the duty cycle to about **18 %**. With <100 photons/m^2/ns/sr, the duty cycle reaches **19.26%**. The other positive effect of such a decision is that the active time consists of much fewer short periods of exposure and much less time lost in manoeuvring the shutter.

References:

1. The Starlink Project, the SLA library. http://star-www.rl.ac.uk/

2. Spacetrack Report No.3, "Models for Propagation of NORAD Elements Sets", F.R. Hoots, R.L. Roehrich, T.S. Kelso et al., 1988 http://www.celestrak.com

3. K. Krisciunas, B.E. Schaefer, Atronomical Society of the Pacific, vol. 103, Sept. 1991, p. 1033-1039.

4. M.R.Dobber “GOME moon measurements, including instrument characterisation and moon albedo” http://earth.esa.int/symposia/papers/dobber/

5. J.M. Anderson, H. Kieffer and K. Becker, "Modeling the brightness of the Moon over 350-2500 nm for spacecraft calibrations", Proc. SPIE 4169, 248-259 (2000)

6. C. Berat, D. Lebrun, A. Stutz, internal report ISN-03-01 – EUSO-SIM-REP-xxx.y.z

7. The COART model: http://snowdog.larc.nasa.gov/jin/rtset.html

8. Tyson and Gal (Astrom J 105 (3) '93